Pergamon

Int. J. Solids Structures Vol. 33, No. 9, pp. 1317–1334, 1996

0020-7683/96 $15.00 + .00

0020-7683(95)00093-3

SHEAR LAG IN ORTHOTROPIC BEAM FLANGES AND PLATES WITH STIFFENERS

R. T. TENCHEV†
Department of Strength of Materials, Sofia Technical University, 1756 Sofia, Bulgaria

(*Received* 1 *August* 1994; *in revised form* 20 *February* 1995)

Abstract—An FEM parametric study of the stress distribution in orthotropic beam flanges was performed. Several beam boundary conditions and cross sections were considered explicitly. The practical variations of cross-sectional dimensions were extended in order to cover the case of thin cover plates with stiffeners. In the FE analyses a two-dimensional plane stress model was used. An empirical formula was established for the shear lag coefficient λ which is used for computing the effective flange width $B_e = \lambda B$ for stress calculations. Longitudinal flange stiffeners can be accounted for by modifying the E/G ratio. The formula is accurate and gives good results even for small T_f/T_w and high E/G ratios, as is the case with fiber reinforced laminated composite plates with stiffeners. Several existing analytical solutions, discussed in the paper, are not reliable for this case.

NOTATION

E	Young's modulus of flange in x direction
G	shear modulus of flange
L	(half) length of beam, Fig. 3
κL	distance between the zero and maximum moment sections, where values of κ are given in Table 1
B	half flange width, Fig. 2
B_e	effective half flange width, defined by eqn (2a)
H	(half) height of web, Fig. 2
T_w	(half) thickness of web, Fig. 2
T_f	(half) thickness of flange, Fig. 2
λ	shear lag coefficient, defined by eqn (2b)
σ_x	normal stress in beam cross section
σ_{xo}	normal stress at web–flange intersection
M_y	bending moment in beam
I_y	moment of inertia of beam cross section
ψ	coefficient to account for flange stiffeners, defined by eqn (8)
x, y, z	Cartesian coordinate system, Fig. 3, Fig. 2b
$S1$–$S4$	beam support cases, Fig. 3
$F1$–$F4$	beam loading cases, Fig. 3

Subscripts

Emp	refer to empirical results
FEM	refer to FEM results

1. INTRODUCTION

According to elementary beam theory (an assumption that plane sections remain plane after bending of the beam) the normal stress σ_x at a point with coordinates (y, z), is:

$$\sigma_x = \frac{M_y}{I_y} z \tag{1}$$

which implies a constant stress in the y direction. In the case of beam cross sections with wide flanges (box, T-, I- cross section) the longitudinal displacements in the parts of the flanges remote from the web (i.e. in the y direction) lag behind those near the web due to the action of in-plane shear strain. This lag results in the distribution of normal stress as

† Visiting researcher at: Mechanics Division, Department of Mathematics, University of Oslo, Norway.

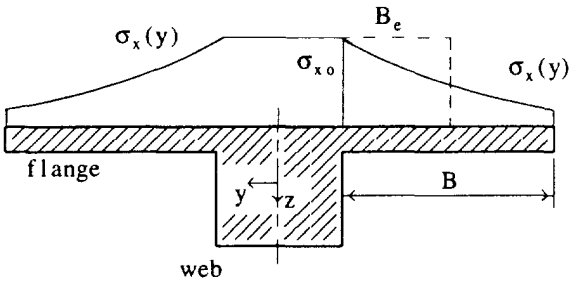

Fig. 1. Shear lag in the cross section of a beam with a wide flange.

shown in Fig. 1. The phenomenon is called shear lag. If the width of the flange is big, eqn (1) will significantly underestimate the stress at the web–flange intersection. However, it is still possible to obtain a correct value for the maximum stress from eqn (1) by using an effective width of the flange B_e:

$$B_e = \frac{1}{\sigma_{xo}} \int_0^B \sigma_x(y)\, dy. \tag{2a}$$

Equation (2a) is of little practical use since $\sigma_x(y)$ is unknown. An alternative formulation is:

$$B_e = \lambda B, \tag{2b}$$

where λ is the shear lag coefficient. The purpose of this paper is to provide a simple way for its calculation.

One of the earliest researches into the shear lag problem has been carried out by von Karmán (1924). It is well documented by Timoshenko and Goodier (1970). An infinitely long continuous beam on equidistant supports is considered. All spans are equally loaded. The width of the flange is infinite. A series solution form of the Airy's stress function for the plane stress field in the flange is chosen to satisfy the boundary conditions. The unknown coefficients are determined by minimizing the strain energy in the beam. However, there is a displacement incompatibility at the flange–web intersection, Vendhan and Bhattacharyya (1987), which leads to an erroneous description of the stress field both for single and multimode solutions. The expression for the effective flange width is correct only for a single-mode solution.

Reissner (1941) assumes a parabolic variation of the bending stress across the width of the flange. A second-order differential equation is obtained for the spanwise variation of the vertex curvature of the stress parabolas. The least work condition is used to determine the unknown quantity. To simplify the solution the work of the transverse normal stresses σ_y is neglected. Simplifications based on the practical variation of cross-sectional dimensions are introduced.

More analytical research into the general shear lag problem has been carried out by Winter (1943), Abdel-Sayed (1969), Malcom and Redwood (1970), Evans and Taherian (1977), Horie *et al.* (1984), Kristek and Evans (1985), Song and Scordelis (1990a,b). Some of the results are discussed later.

The shear lag effect in box girders of varying depth has been addressed by Chang and Yun (1988); in cantilever beams with a trapezoidal box cross-section—by Dezi and Mentrasti (1985). The prestress influence on shear lag effect in continuous box girder bridges—by Chang (1992).

Apparently the analytical research could not provide a general, reliable and suitable-for-design-purposes solution of the shear lag problem and a specialized computer program for the analysis of box girder bridges, based on the finite element method, has been developed by Hinton and Hewitt (1975).

Moffatt and Dowling (1972, 1975) have performed a comprehensive parametric FEM study on shear lag in steel box girders. Their results were used as a basis for the formulation of the British shear lag rules, Moffatt and Dowling (1978).

A brief survey yields the following conclusions:

(1) For a given problem (e.g. a simple beam, uniform load, box cross section) there are several analytical solutions (cited above) for the shear lag effect, due to the different initial assumptions. To simplify the results and to make them useful to the design engineer more assumptions and approximations are introduced and, usually, there is no information about the error involved. Explicit results for beams with a variety of support and loading conditions are rarely presented.

(2) FEM results are considered more reliable than analytical solutions (the British shear lag rules are based on FEM results).

(3) For beams whose flanges are made from laminated fibre reinforced composites the E/G ratio has a significant influence on the shear lag. Design codes (Moffatt and Dowling, 1978; Thein Wah, 1960) deal only with beams made from isotropic material (steel). Even a code for fibre composite and sandwich constructions (Det Norske Veritas, 1991) makes no provisions for varying E/G. Reissner (1941), Horie *et al.* (1984) and Kristek and Evans (1985) presented solutions for cantilever and simple beams depending on E/G. The solutions include beam cross-sectional dimensions and extending their application beyond the practical variation of these dimensions is questionable. For example, for a beam cross section usually $T_f/T_w \geqslant 1$ but when a fibre reinforced composite plate with stiffeners is considered (Fig. 2e) then it is possible that $T_f/T_w \approx 0.1$.

2. PARAMETRIC STUDY

An empirical formula which is to be used for design purposes (i.e. for the sake of simplicity some error is allowed) may neglect some parameters.

The parameters on which shear lag depends must be defined:

(a) *Loading and supports*

It is well known (Reissner, 1941; Moffatt and Dowling, 1972, 1975; Roark and Young, 1975; Kristek and Evans, 1985; Song and Scordelis, 1990a) and confirmed by the present FEA that shear lag depends on loading and support conditions.

(b) B/L *and* E/G

The dependence of shear lag on the B/L and E/G ratios is well known (Reissner, 1941; Moffatt and Dowling, 1972, 1975; Roark and Young, 1975; Horie *et al.*, 1984; Kristek and Evans, 1985) and confirmed by the present FEA (Fig. 5). Some researchers (von Karmán, 1924; Song and Scordelis, 1990a,b), however, restrict their analysis to isotropic materials and Poisson's ratio is used instead of E/G.

(c) *Web dimensions, flange thickness*

There is not a fixed opinion on the sensitivity of shear lag on these parameters. Von Karmán's (1924) solution, when the bending moment is in the form $M \cos \pi x$, is independent of these dimensions. Reissner (1941) included a ratio m defined by the moment of inertia of the web(s) and flange(s) in his analysis and final results. However, it is reported in Roark and Young (1975) that for the practical range of m the variation in the shear lag is small enough to be disregarded. Horie *et al.* (1984) and Moffatt and Dowling (1975, 1978) concluded that the shear lag may be regarded as independent of these dimensions for uniform loading but for a concentrated load their effect is not negligible.

FEA showed that varying web height H in reasonable margins ($H < 0.5L$ and $H > 10T_f$) and different values of T_f and T_w (but constant ratio T_f/T_w) have practically no effect on the shear lag. However, the ratio T_f/T_w, when it is varied in wide margins ($0.05 < T_f/T_w < 5.0$), causes variation of λ up to 30%. The lower values of T_f/T_w may apply for plates with longitudinal stiffeners, when the stiffener (with box or I- cross section)

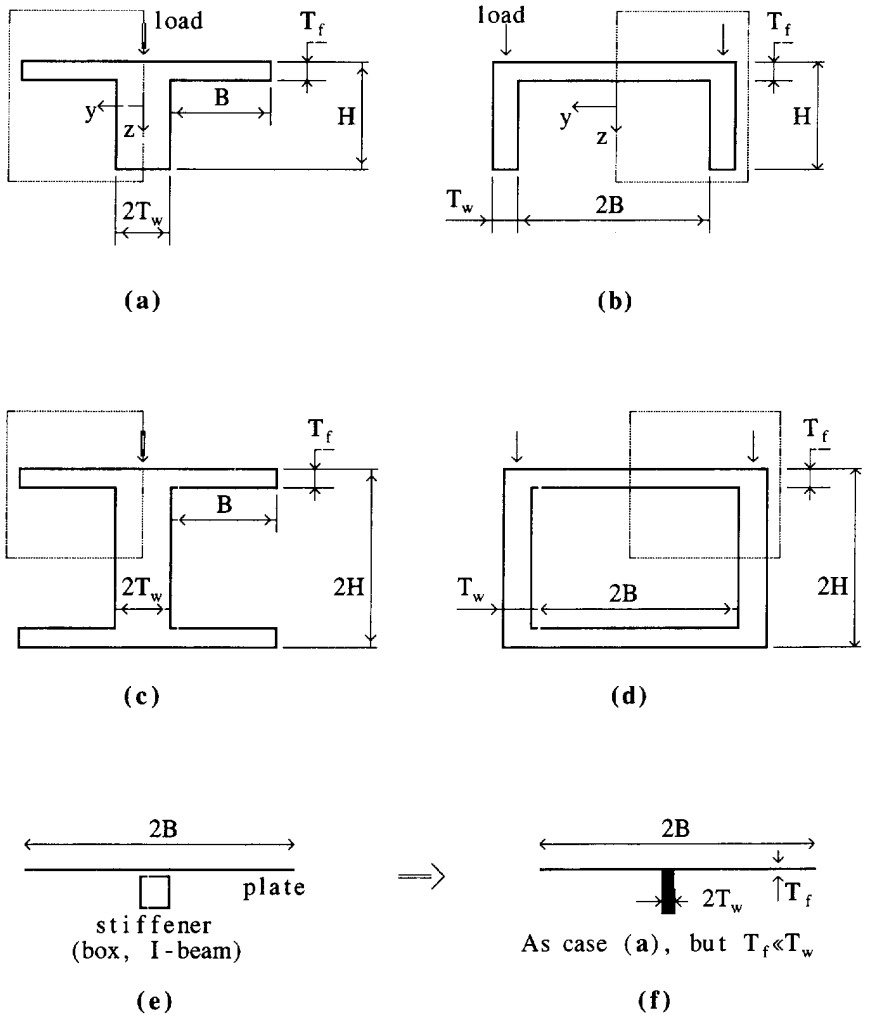

Fig. 2. Cross sections used in the shear lag analysis. (a),(b),(c),(d)—T-, U-, I- and box cross sections, respectively, (e) thin plate with a stiffener (box, I-, etc.), (f) equivalent model: T- section, as case (a) but $T_f \ll T_w$. Dotted rectangular—the part for FEM analysis (due to symmetry).

is replaced by an equivalent (i.e. having the same moment of inertia and preserving the position of the centroid, Fig. 2e) rectangular web.

(d) *Type of cross section*

The shear lag may be considered independent of the type of cross section (box, T-, I- or U-); Winter (1943), Roark and Young (1975), Moffatt and Dowling (1975, 1978), Song and Scordelis (1990). FEA confirmed this conclusion.

(e) *Variation of* E_y, ν_{xy} *of flange*

FEA show that those parameters have negligible influence on the shear lag. Reissner (1941) neglects the work done by the transverse normal stresses σ_y in the flange, which amounts to putting $E_y = \infty$ and $\nu_{xy} = 0$.

(f) *Material properties of the web*

For the practical values of the dimensions of the cross section the shear stress/strain in the web can be neglected. Von Karmán (1924) and Reissner (1941) take into account only the normal stresses σ_x when computing the strain energy in the web. The material of the web may be treated as isotropic and changing its material properties, i.e. Young's

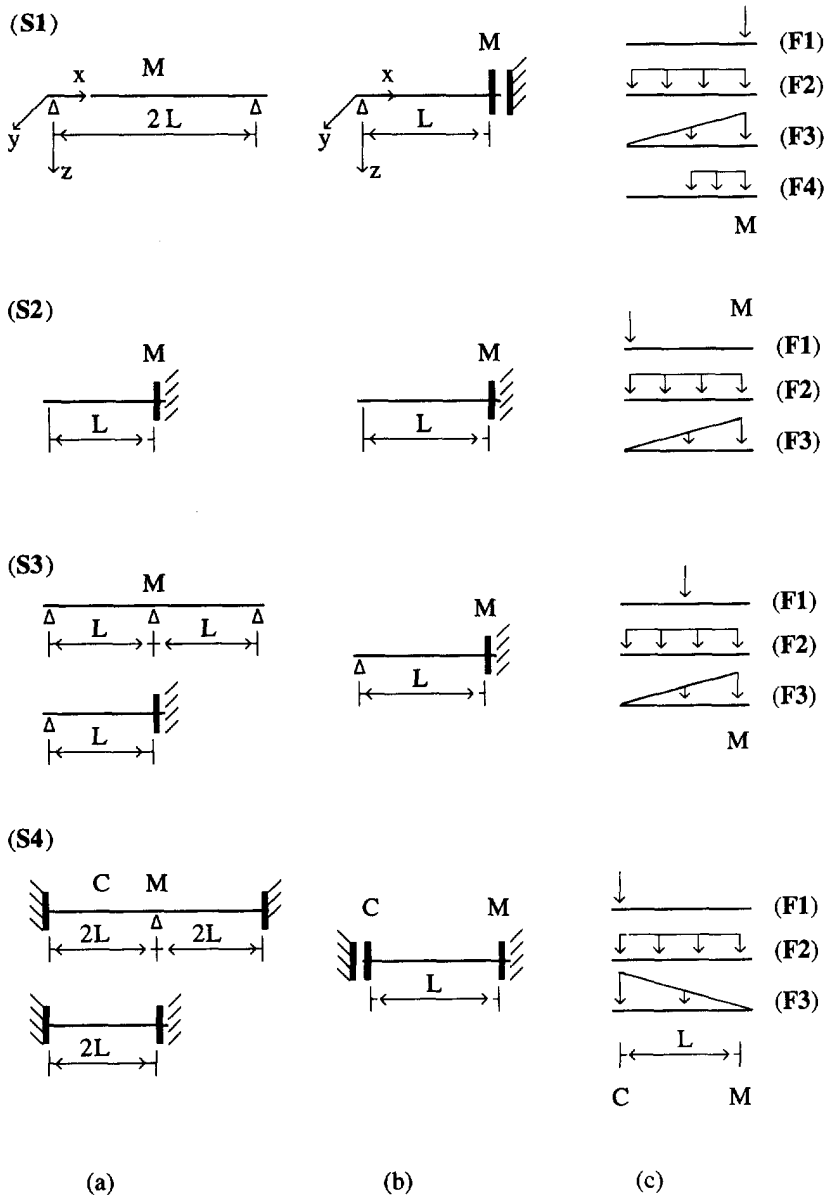

Fig. 3. (a) Full beam, (b) beam to be analyzed when symmetry is taken into account, (c) load cases applied on beam model (b); $F1$—concentrated, $F2$—uniform, $F3$—linear load.

modulus, is equivalent to changing the thickness of the web. Then the considerations in part (c) apply.

The aim of this paper is to produce an easy-to-use formula for the calculation of the shear lag coefficient λ. From the presented parametric study it is concluded that the formula must take into account:

(a) the loading and the support conditions;
(b) the ratios B/L, E/G and T_f/T_w.

Since it is basically for design purposes, the analysis will be restricted only to the cross section with the maximum bending moment, i.e. the variation of λ along the span of the beam will not be considered.

3. THE FEM MODEL

Several beams, shown in Fig. 3a, are considered. Taking into account symmetry, the beam models to be analyzed are shown in Fig. 3b. Only beams with a symmetrical cross

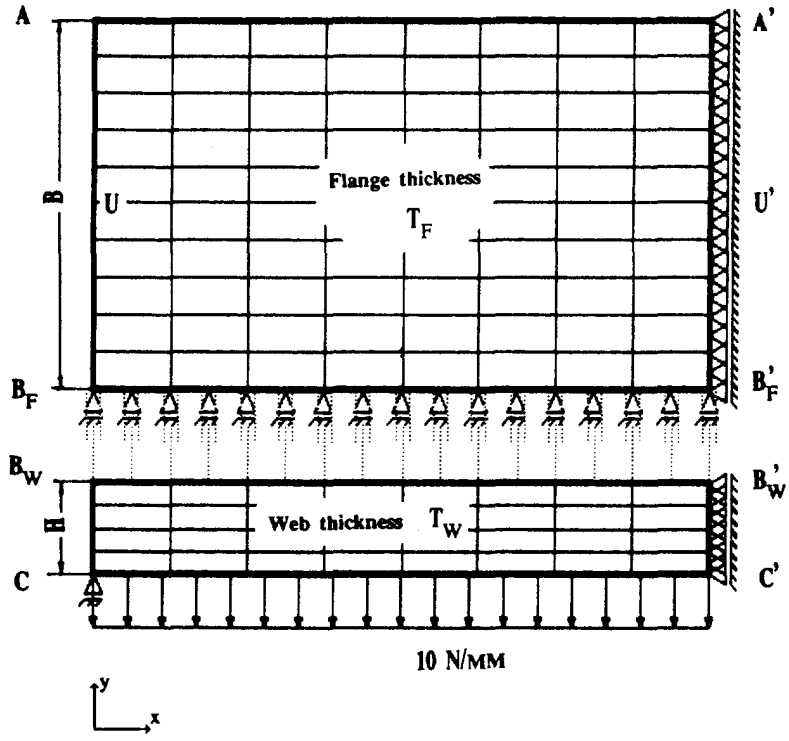

Fig. 4. The two-dimensional plane stress FEM model for half of a simple beam (case *S1–F2* in Fig. 3b) with T- cross section. Lines B_f–B_f' and B_w–B_w' have equal displacements along x.

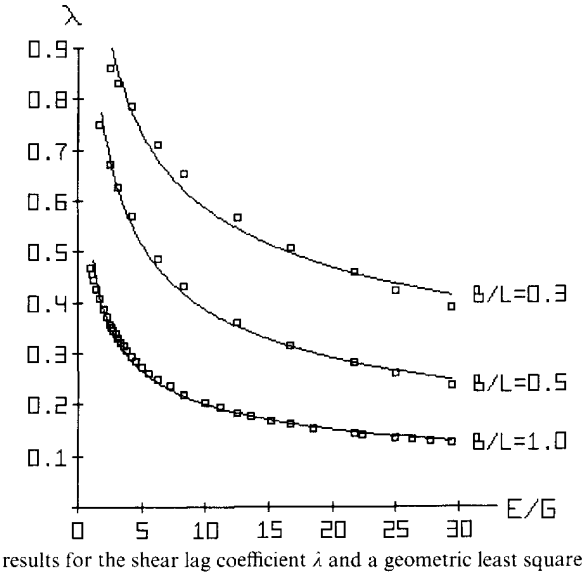

Fig. 5. FEM results for the shear lag coefficient λ and a geometric least square interpolation.

section (box, T-, I- and U-, shown in Fig. 2) and loading in the plane(s) of the web(s) are considered. Due to symmetry, a half or a quarter of the cross section is modeled (shown by the broken line rectangles in Fig. 2). This results in identical FEM meshes with only different boundary conditions to account for the missing parts.

For the FEM model the straightforward choice is to use three-dimensional shell or solid elements. However, since a large number of FE analyses are required, special attention was paid to reducing computer effort without reducing the accuracy of the results. The tradition in shear lag analysis (von Karmán, 1924; Reissner, 1941; Kristek and Evans, 1985; Song and Scordelis, 1990a) is to assume that flange thickness T_f is very small in

comparison to the web height H. Bending of the flange as a thin plate can then be neglected, and it can be assumed that during bending of the beam the forces are transmitted to the flange in its middle plane so that the stress distribution in the flange presents a two-dimensional plane stress problem. The stress distribution in the web is two-dimensional, too. The only reason to use three dimensional FEA is that the two planes (flange and web) are mutually perpendicular. However, in the FEM model it is possible to rotate either the flange or web and make them co-planar (Tenchev, 1994) and to use two-dimensional plane stress elements.

The two-dimensional plane stress FEM model of a uniformly loaded simple T-beam (case *S*1-*F*2, Fig. 3), when symmetry is taken into account, is shown in Fig. 4. Rectangle $B_W B'_W CC'$ represents the web and rectangle $AA'B'_F B_F$—the flange, which is rotated 90° about the x axis. Lines A'–B'_F and B'_W–C' are at the mid-span of the beam (the plane of symmetry) and all nodes on those lines have x displacements set to zero. The left support of the simple beam is at point C and the corresponding node has y displacement set to zero. A constraint is imposed that corresponding nodes on lines B_W–B'_W and B_F–B'_F have equal x displacements. Those lines coincide in the real problem and represent the web–flange intersection. In the two-dimensional model the distance between them is arbitrary. The constraint provides the load transfer from the web to the flange. Line B_F–B'_F has y displacement set to zero which accounts for the symmetry of the cross section, i.e. the beam does not deflect in the y direction in Fig. 2. The load is applied along the web either on line B_W–B'_W or line C–C' (or any line in the web parallel to them).

In the case of I- and box cross sections (i.e. when y is an axis of symmetry, Fig. 2) the x displacements of all nodes on line C–C' (the neutral line) are set to zero. In the case of U- and box cross section (i.e. when z is an axis of symmetry) the y displacements of all nodes on line A–A' are set to zero.

In the present study local effects of concentrated forces will not be accounted for and in the two-dimensional FEM model a concentrated load is represented as a constant distributed load applied along the height of the web (on line B'_W–C', Fig. 4).

In a real three-dimensional model, for a given cross section, the deflection z of a point at the web–flange intersection is different from the deflection of a point at the end of the flange. This is not accounted for by the two-dimensional model. FEM three-dimensional shell analyses show that: (a) in the case of pin supports (simple beam, etc., when the beam cross section at the support is not restricted to deform out of plane) the stresses at the maximum moment cross section are identical to those computed by the two-dimensional model; (b) in the case of built-in supports (i.e. the cross section is forced to remain plane) the difference in the stresses is negligible.

The FEM program was developed by the author and extensively tested in the course of several years. Quadratic (eight nodes), isoparametric plane stress elements were used. The constraint is modeled by stiff bar elements connecting the corresponding nodes on lines B_W–B'_W and B_F–B'_F in the x direction. The bar elements are assembled last and they are assigned high relative stiffness—about 10^6 times higher than the corresponding stiffness coefficients at the main diagonal of the global stiffness matrix. Such values result in practically identical x displacements of the corresponding nodes on lines B_W–B'_W and B_F–B'_F and cause no numerical difficulties when double precision mathematics is used.

In the cases of a distributed load (*F*2–*F*4, Fig. 3c) the mesh is uniform, as shown in Fig. 4. The flange and web are modeled by 80 and 32 elements, respectively. In the cases of a concentrated load (*F*1, Fig. 3c), the column of elements where the load is applied (Line A'–C', Fig. 4) is divided into two and the number of elements is 90 and 36. A convergency study showed that those meshes are sufficiently accurate. A test problem was solved: simple T-beam; uniform distributed load $q = 10$ N mm^{-1}; isotropic material $E/G = 2.5$; beam length $L = 200$ mm (Fig. 3, case *S*1); dimensions of the cross section (Fig 2a) $B = 100$ mm, $H = 25$ mm, $T_w = 10$ mm, $T_f = 1$ mm. The computed maximum normal stress at the web–flange intersection (point B'_F, Fig. 4) is $\sigma_x = -90$ N mm^{-2}. At the end of the flange, point A', $\sigma_x = -43.4$ N mm^{-2}.

A regression analysis showed that σ_x distribution in the flange is quadratic and Reissner's (1941) assumption is accurate.

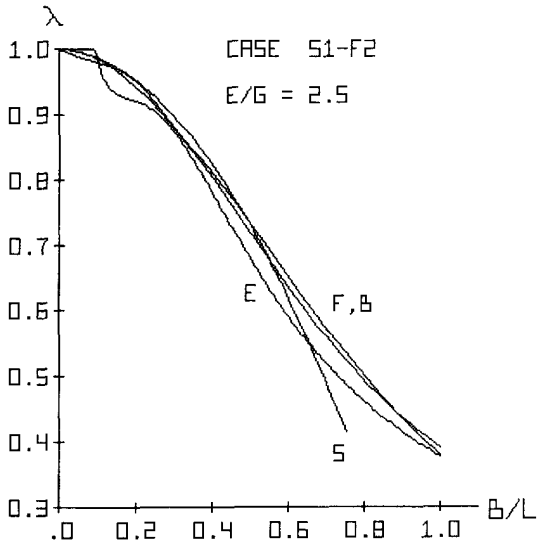

Fig. 6. Comparison of shear lag coefficient. λ. Case $S1$–$F2$ (simple beam, uniform load); $E/G = 2.5$, $T_f/T_w = 1.0$. F—Finite element results; E—empirical formula, eqn (4); B—British shear lag rules, Moffatt and Dowling (1978); S—Song–Scordelis (1990b).

The FEM shear lag coefficient is computed according to eqns (2a,b):

$$\lambda_{\text{FEM}} = \frac{1}{B\sigma_{x0}} \int_0^B \sigma_x(y)\,\mathrm{d}y. \tag{3}$$

4. EMPIRICAL FORMULA FOR THE SHEAR LAG COEFFICIENT λ

FEM results for the shear lag coefficient when E/G is varied are approximated by a geometric least square fit in Fig. 5. It can be clearly seen that the approximation is quite accurate. Similar graphs are obtained when B/L and T_f/T_w are varied. These findings are crucial to the success of the empirical approach and mean that a multi-variable geometric least square fit may be applied.

Test problems which must provide the experimental data (i.e. FEM results) are generated as follows: the span $L = 500$ mm of a T-beam is fixed; E/G is varied from 1.0 to 30 on eight steps; B/L is varied on eight steps from 1.0 to 0.1 when $E/G = 1.0$ and from 0.6 to 0.03 when $E/G = 30$ (for the intermediate values of E/G a linear interpolation for the maximum and minimum values of B/L is used); T_f/T_w is varied from 0.05 to 3.0 on five steps; T_w is varied on two steps; $0.05H$ and $0.02H$; $H = 0.5B$ is fixed. Two conditions are satisfied: (a) an assumption of small flange thickness, i.e. $T_f \leqslant 0.1H$ (if $T_f > 0.1H$ then $T_f = 0.1H$); (b) beam theory to be valid—$H \leqslant 0.25L$ (if $H > 0.25L$ then $H = 0.25L$). As a result 640 problems are automatically generated and solved for each case of support and loading conditions (Fig. 3, total of 13 cases).

After inspecting the results, the following expression for the empirical evaluation of shear lag coefficient λ is proposed:

$$\lambda_{\text{Emp}} = \frac{p}{C_1 C_2} \left(\frac{B}{\kappa L}\right)^q \left(\frac{E}{G}\right)^r \left(\frac{T_f}{T_w}\right)^S \tag{4}$$

$$\text{if} \quad \lambda_{\text{Emp}} > 1 \quad \lambda_{\text{Emp}} = 1 \tag{4a}$$

where

Table 1. Values of the coefficients in eqn (4). The code for beam and load is according to Fig. 3

Beam	Load	κ	p	q	r	s	t	u	v
$S1$	$F1$		0.384	−0.834	−0.389	−0.040	3.1	0.3	−1.0
	$F2/F4$	1	0.570	−0.850	−0.416	0.0	5.0	0.31	−0.9
	$F3$		0.542	−0.866	−0.422	0.0			
$S2$	$F1$		0.397	−0.818	−0.387	−0.037	3.0	1.1	−2.0
	$F2$	1	0.282	−0.831	−0.376	−0.062	2.0	2.0	−3.0
	$F3$		0.228	−0.858	−0.379	−0.073	1.7		
$S3$	$F1$	0.273	0.463	−0.945	−0.434	−0.011			
	$F2$	0.250	0.449	−0.942	−0.425	−0.019	4.0	0.0	0.0
	$F3$	0.226	0.446	−0.951	−0.419	−0.021			
$S4$	$F1$	0.500	0.435	−0.871	−0.429	−0.022	3.0		
	$F2$	0.424	0.417	−0.883	−0.423	−0.033	3.2	0.0	0.0
	$F3$	0.384	0.496	−0.879	−0.429	−0.027	4.5		

$$C_1 = 1 + te^X, \quad X = -6.4\frac{B}{\kappa L}\sqrt{\frac{E}{G}} \tag{4b}$$

$$C_2 = 1 + ue^{rY}, \quad Y = \left(\frac{E}{G}\right)\left(\frac{B}{\kappa L}\right)^{-1} \tag{4c}$$

C_1, C_2—coefficients to enhance the approximation at the extremities of B/L and E/G; $e = 2.7183$ is the base of the natural logarithm; p, q, r, s, u, t, v—coefficients to be determined from a least square fit; κL—distance between the zero moment and the maximum moment cross section. Values of κ are given in Table 1.

At the maximum moment cross section for all considered cases $\lambda_{FEM} \leqslant 1$.

In eqn (4a) $\lambda_{Emp} > 1$ is due to an error of the fitting procedure. It does not imply a shear lag anomaly, Foutch and Chang (1982), or a negative shear lag, Kristek and Studnicka (1991).

The unknown coefficients are determined from a least square fit. The results are presented in Table 1. The support conditions $S1$–$S4$ and loading $F1$–$F4$ are given in Fig. 3. The shear lag coefficient λ_{Emp} is valid for the maximum moment cross section along the span of the beam and for types of cross sections given in Fig. 2.

For all considered problems when the maximum value of B/L is used (i.e. $\max(B/L) = 1.0$ when $E/G = 1.0$, $\max(B/L) = 0.6$ when $E/G = 30$, etc.) the normal stress σ_x in the part of the flange most distant from the web(s) is practically zero. So, if in practice $B/L > \max(B/L)$ then $B/L = \max(B/L)$ may be used for either FEA or empirical calculations without introducing any error.

5. ACCURACY OF λ_{Emp}

5.1. *Errors of the fitting procedure—comparison with FEA results*

The error of $\lambda_{Emp,i}$ for the ith solved problem is:

$$\Delta\lambda_i = \frac{\lambda_{Emp,i} - \lambda_{FEM,i}}{\lambda_{FEM,i}} 100\%. \tag{5}$$

The mean square error $\Delta\lambda_{MSq}$ when N problems are solved may be considered as an

Table 2. Errors (%): maximum, minimum (maximum negative) and mean square for the shear lag coefficient λ. Column A—accuracy of the fit, column B—comparison with new FEM results

Beam	Load	A max $\Delta\lambda$	A min $\Delta\lambda$	A $\Delta\lambda_{MSq}$	B max $\Delta\lambda$	B min $\Delta\lambda$	B $\Delta\lambda_{MSq}$
S1	*F1*	6.91	−8.84	3.47	7.15	−9.76	3.45
	F2	5.92	−6.40	2.88	6.42	−5.42	2.67
	F3	4.97	−6.26	2.60	4.85	−5.29	2.20
	F4	5.88	−6.53	2.87	9.84	−4.03	4.53
S2	*F1*	7.75	−8.66	3.48	8.16	−7.21	3.48
	F2	8.85	−10.47	4.21	9.34	−12.16	4.36
	F3	11.64	−12.96	4.66	12.48	−13.67	4.88
S3	*F1*	8.46	−8.66	3.88	9.85	−11.20	4.90
	F2	9.76	−11.76	4.47	10.26	−14.96	5.36
	F3	10.18	−12.37	4.72	11.67	−15.77	6.11
S4	*F1*	7.72	−7.93	3.25	8.03	−9.94	3.37
	F2	6.77	−9.49	2.95	7.15	−13.11	3.48
	F3	7.60	−8.62	3.16	7.45	−12.08	3.38

overall measure of the accuracy:

$$\Delta\lambda_{MSq} = \sqrt{\frac{1}{N}\sum_{i=1}^{N}(\Delta\lambda_i)^2}. \tag{6}$$

The maximum, minimum (i.e. maximum negative) and the mean square errors of the empirical fit to the FEM results (those used for the least square fit, $N = 640$) are given in Column A of Table 2.

New test problems, generated by the same procedure described in Section 4, are solved with different values of the parameters: $L = 5000$ mm; $H = 0.3B$ and $H = 0.7B$; $T_w = 0.06B$ and $T_w = 0.03B$; T_f varied from $0.07T_w$ to $2.5T_w$ on four steps; E/G and B/L are varied on six steps giving intermediate values to those used in the previous section. The same restrictions to the dimensions, mentioned in the previous section, are applied. The total number of generated and solved problems for each case in Fig. 3 is $N = 553$. These results are not used in the least square fit. The errors are presented in Column B of Table 2.

The maximum errors in all cases occur near the extremities of the variation of B/L, E/G and T_f/T_w. For most practical problems one may expect an error close to the mean square error. Having in mind that the empirical formula, eqn (4) and Table 1, is to be used for design calculations the errors are considered acceptable.

5.2. *Comparison with other formulas*

To check the performance of the proposed empirical formula, the following test problems are considered:

(a) test problem *S1–F2*: (simple beam, uniform load) $2L = 200$ cm.
(b) test problem *S2–F2*: (cantilever beam, uniform load) $L = 200$ cm.

In both cases it is a box cross section with $2H = 25$ cm and $T_w = 2$ cm. Two values for the flange thickness are considered: $T_f = 2$ cm (i.e. $T_f/T_w = 1$, a typical value for a beam box section, Fig. 2d) and $T_f = 0.2$ cm (i.e. $T_f/T_w = 0.1$, a typical value for a plate with stiffeners, Fig. 2e). Two values of E/G are considered: $E/G = 2.5$ (isotropic material with Poisson's ratio 0.25) and $E/G = 25$ (a typical value for carbon fibre/epoxy composites). The B/L ratio is varied from 0.05 to 1.0 on 20 steps.

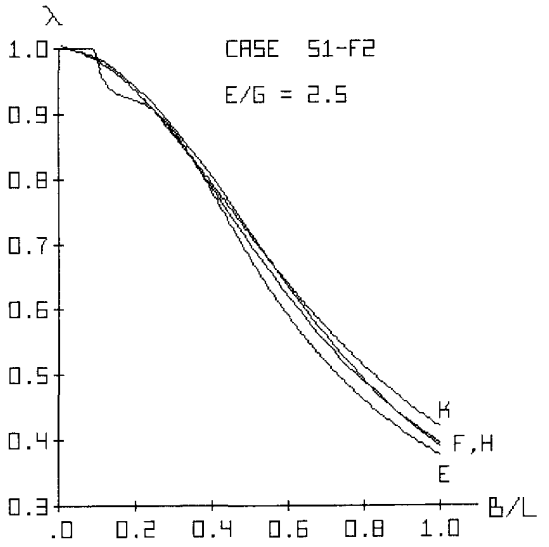

Fig. 7. Comparison of shear lag coefficient λ. Case $S1$–$F2$ (simple beam, uniform load); $E/G = 2.5$, $T_f/T_w = 1.0$. F—Finite element results; E—empirical formula, eqn (4); H—Horie *et al.* (1984); K—Kristek and Evans (1985).

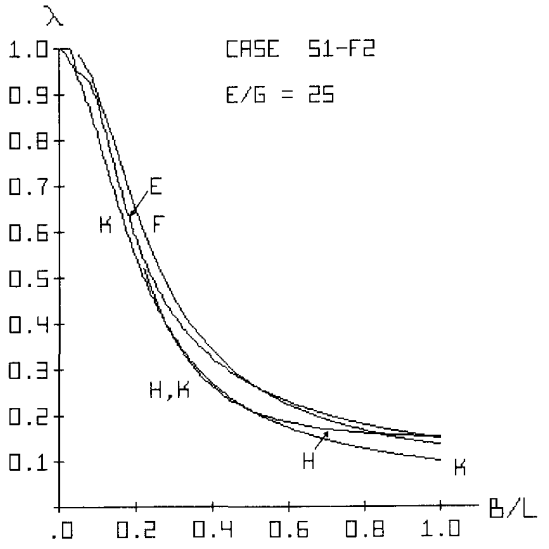

Fig. 8. Comparison of shear lag coefficient λ. Case $S1$–$F2$ (simple beam, uniform load); $E/G = 25.0$, $T_f/T_w = 1.0$. F—Finite element results; E—empirical formula, eqn (4); H—Horie *et al.* (1984); K—Kristek and Evans (1985).

In Figs 6–12 graphs "F" are based on the FEM computation of λ, eqn (3); graphs "E" on the empirical formula, eqn (4); graphs "B" (British shear lag Rules) on Moffatt and Dowling's (1978) tabulated results; graph "S" on Song and Scordelis (1990b); graphs "H" on Horie *et al.* (1984); graphs "K" on Kristek and Evans (1985). Kristek and Evans' (1985) formula gives the true stress at the web–flange intersection when shear lag is taken into account. The corresponding shear lag coefficient is calculated from this stress and using eqns (1) and (2b).

In Figs 6 and 7 results for the shear lag coefficient λ for test problem $S1$–$F2$ with $E/G = 2.5$ and $T_f/T_w = 1$ are shown. Song and Scordelis's (1990b) formula, graph "S" in Fig. 6, is said to be valid for $B/L < 0.5$ but it can be seen that an extension to 0.75 is acceptable. In Fig. 8 the same problem is solved but $E/G = 25$. Horie's formula (graph "H") uses coefficients which are complicated functions of the dimensions of the cross

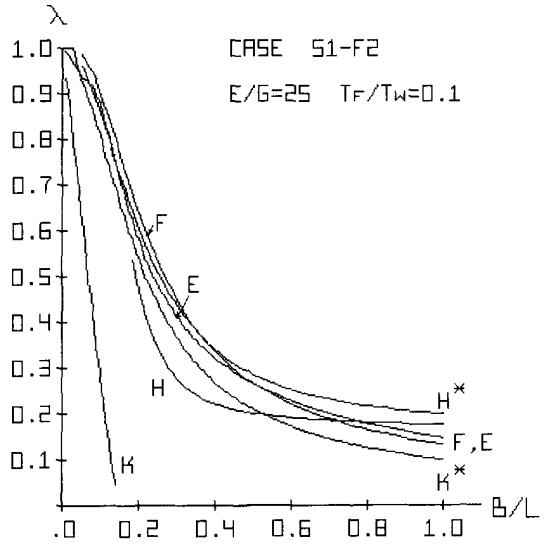

Fig. 9. Comparison of shear lag coefficient λ. Case $S1$–$F2$ (simple beam, uniform load); $E/G = 25.0$, $T_f/T_w = 0.1$. F—Finite element results; E—empirical formula, eqn (4); H—Horie *et al.* (1984); K—Kristek and Evans (1985).

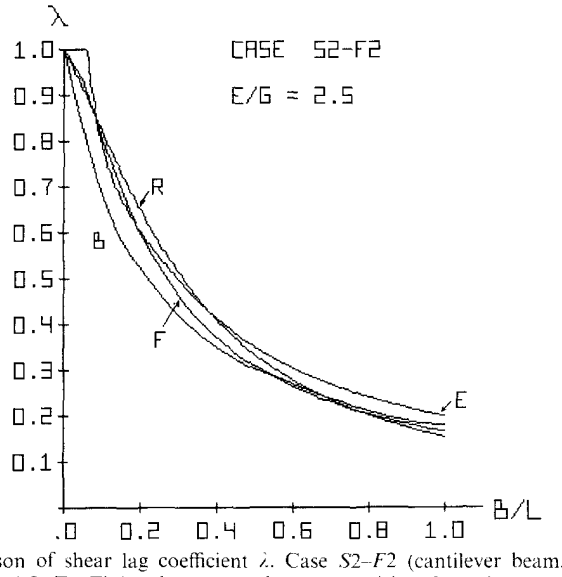

Fig. 10. Comparison of shear lag coefficient λ. Case $S2$–$F2$ (cantilever beam, uniform load); $E/G = 2.5$, $T_f/T_w = 1.0$. F—Finite element results; E—empirical formula, eqn (4); R—Reissner [1941, eqn (55)] in his paper; B—British shear lag rules. Moffatt and Dowling (1978).

section (parameters B/H and T_f/T_w) and for small values of B/H ($B/H < 1.5$, i.e. $B/L < 0.19$) the formula fails because a square root of a negative number must be calculated.

The empirical formula was established for $B/L < 0.6$ when $E/G = 25$, but it can be seen that the accuracy is good for $0.6 \leqslant B/L \leqslant 1.0$.

There is good agreement among all results.

Variation of H and increasing T_f/T_w have a negligible effect on all graphs in Figs 7 and 8. Graph "S" in Fig. 6 is independent of cross-sectional dimensions. In Fig. 7 ($E/G = 2.5$) decreasing T_f/T_w to $T_f/T_w = 0.1$ has a negligible effect on Horie's formula and small deterioration of Kristek and Evans' results.

In Fig. 9 results of test problem $S1$–$F2$ with $E/G = 25$ and $T_f/T_w = 0.1$ are shown. The reduced ratio $T_f/T_w = 0.1$ is not typical for a beam cross section. If web height H is decreased by the same amount as flange thickness (i.e. 10 times), thus preserving the ratio (flange area)/(web area), Kristek and Evans' formula (graph "K*") and Horie's formula (graph

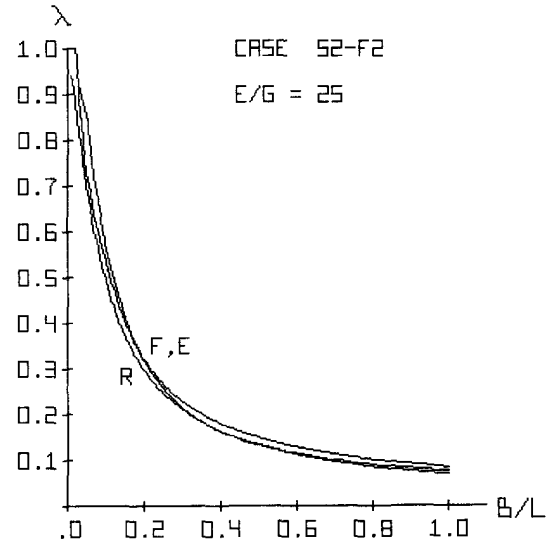

Fig. 11. Comparison of shear lag coefficient λ. Case $S2$–$F2$ (cantilever beam, uniform load); $E/G = 25.0$, $T_f/T_w = 1.0$. F—Finite element results; E—empirical formula, eqn (4); R—Reissner [1941, eqn (55)].

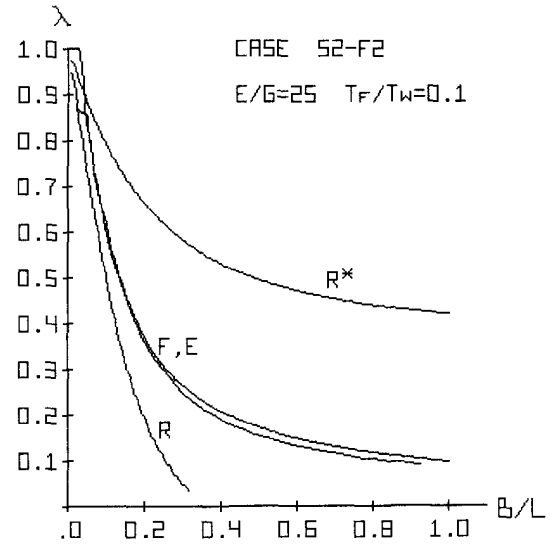

Fig. 12. Comparison of shear lag coefficient λ. Case $S2$–$F2$ (cantilever beam, uniform load); $E/G = 25.0$, $T_f/T_w = 0.1$. F—Finite element results; E—empirical formula, eqn (4); R—Reissner [1941, eqn (55)—simplified formula]; R*—Reissner [1941, eqn (50)—non-simplified formula].

"H*") are in good agreement with "F" and "E" graphs. If, however, web height is not changed, the accuracy of Horie's formula (graph "H") deteriorates for small B/L and Kristek and Evans' formula (graph "K") is much in error.

In Fig. 10 results for test problem $S2$–$F2$ with $E/G = 2.5$ and $T_f/T_w = 1$ are shown. All results are in good agreement. Changing T_f/T_w to $T_f/T_w = 0.1$ has negligible effect on the "R", "E" and "F" graphs. The "B" graph comes from tabulated data and is not dependent on cross-sectional dimensions.

In Figs 10 and 11 results for test problem $S2$–$F2$ with $E/G = 2.5$ and $E/G = 25$, respectively, and $T_f/T_w = 1$ are shown. Reissner's [1941, eqn (55)] results are in good agreement with the other results.

In Fig. 12 the same problem is analyzed but with $T_f/T_w = 0.1$. Reissner's (1941) formula, eqn (55) in his paper, makes use of two approximations to hyperbolic functions which are valid for the practical range of beam cross-sectional dimensions. But with

Table 3. Comparison of max σ_x and λ; steel box girder, without stiffeners, simply supported, uniform load

	Kristek and Evans (1985)	Moffatt and Dowling (1975)	FEM (Fig. 4)	Empirical [eqn (4)]
σ_x	−69.0 MPa	−68.9 MPa	−70.6 MPa	−71.9 MPa
λ	0.807	0.810	0.798	0.777

$T_f/T_w = 0.1$ this is not the case and the deterioration of the results is evident. Graph "R*" represents the results from his non-simplified formula [eqn (50) in his paper]. Both formulas use a dimensionless parameter which is a function of the moments of inertia of the web(s) and the flange(s). The non-simplified formula is practically insensitive to variation of cross-sectional dimensions but the agreement with FEM results is not very good.

Kristek and Evans (1985) have solved an example: simple beam, span $2L = 9144$ mm, uniform load $q = 1$ kN mm^{-1}, box cross section with dimension (according to Fig. 2d) $2H = 1829$ mm, $2B = 3632.6$ mm, $T_f = 25.4$ mm, $T_w = 12.7$ mm, isotropic material (steel). A comparison of some results is made in Table 3. There is good agreement among them. The error of the empirical formula eqn (4), when compared to FEM, is $|\Delta\lambda| = |-2.7\%|$ and it is close to the mean square error given in Table 2.

From these comparisons it may be concluded that:

(a) For the practical range of beam cross-sectional dimensions and E/G ratio there is good agreement for the shear lag coefficient λ between analytical solutions (Reissner, 1941; Horie *et al.*, 1984; Kristek and Evans, 1985; Song and Scordelis, 1990b), FEM solutions (Moffatt and Dowling's, 1978; present FEA) and the empirical formula, eqn (4). For isotropic materials ($E/G \approx 2.5$) and small T_f/T_w ratio (steel plates with stiffeners) there is good agreement of all results, too.

(b) In the cases of small T_f/T_w ratio and high E/G ratio (fibre reinforced laminated composite plates with stiffeners) the analytical solutions are not reliable. The empirical formula, eqn (4), provides good accuracy for design purposes.

6. EXTENDED APPLICATIONS

6.1. *Flange with longitudinal stiffeners*

Longitudinal stiffeners in a beam cross section contribute to the axial stiffness of the flange and have negligible effect on the shear stiffness. In this case the shear lag is more pronounced (Fig. 5, increasing E/G ratio).

Due to the stiffeners, the axial stiffness of the flange will be increased by a factor ψ:

$$\psi = \frac{AE + A_s E_s}{AE} \tag{7}$$

where A_s is the stiffeners total cross-sectional area at each flange; E_s is Young's modulus of stiffeners and A, E are the cross-sectional area and Young's modulus of the flange, respectively.

In eqn (4) instead of (E/G) the modified ratio $(\psi E/G)$ must be used.

Kristek and Evans (1985) have solved an example: simple beam, span $2L = 9144$ mm, uniform load $q = 1$ kN mm^{-1}, box cross section with dimension (according to Fig. 2d) $2H = 1829$ mm, $2B = 3632.6$ mm, $T_f = 12.7$ mm, $T_w = 12.7$ mm, isotropic material (steel). Total cross-sectional area of the stiffeners on each flange $A_s = 46456.6$ mm^2.

For this problem $\psi = 2$ and comparison of some results is made in Table 4.

For the FEM model the total area of the stiffeners A_s is assumed to be distributed uniformly along the flange width and the new flange thickness is $t_f + A_s/2B$. Young's modulus for the flange and the web is $E = 2 \times 10^5$ N mm^{-2}, Poisson's ratio $\nu = 0.3$, the web is isotropic and the flange is assumed to be orthotropic with shear modulus

Table 4. Comparison of max σ_x and λ; steel box girder, with stiffeners, simply supported, uniform load

	Kristek and Evans (1985)	Moffatt and Dowling (1975)	FEM (Fig. 4)	Empirical [eqn (4)]
σ_x	−83 MPa	−82 MPa	−84.4 MPa	—
λ	—	0.67	0.65	0.62

$$G = \frac{1}{\psi}\frac{E}{2(1+\nu)} = 0.385\,\mathrm{N\,mm^{-2}}.$$

There is again good agreement among the results.

6.2. *Load combination*

In the case of load combinations, using the principle of superposition, the shear lag coefficient is:

$$\lambda^{\mathrm{I+II+}\ldots} = \frac{1}{\sigma^{\mathrm{I}}_{xo}+\sigma^{\mathrm{II}}_{xo}+\ldots}\frac{1}{B}\int_0^B (\sigma^{\mathrm{I}}_x(y)+\sigma^{\mathrm{II}}_x(y)+\ldots)\,\mathrm{d}y \tag{8}$$

or:

$$\lambda^{\mathrm{I+II+}\ldots} = \frac{\lambda^{\mathrm{I}}\sigma^{\mathrm{I}}_x(\lambda^{\mathrm{I}})+\lambda^{\mathrm{II}}\sigma^{\mathrm{II}}_x(\lambda^{\mathrm{II}})+\ldots}{\sigma^{\mathrm{I}}_x(\lambda^{\mathrm{I}})+\sigma^{\mathrm{II}}_x(\lambda^{\mathrm{II}})+\ldots}. \tag{8a}$$

Superscripts I, II, etc. refer to the corresponding load case when solved separately and $\sigma_x(\lambda)$ is the constant stress in the flange, given by eqn (1), when the effective flange width, eqn (2b), is used. Equation (8a) is to be used when the section with the maximum moment remains the same for each load case as well as for the total load combination. A necessary condition is that $\sigma^{\mathrm{I}}_x, \sigma^{\mathrm{II}}_x$, etc. have equal signs. When the stresses have opposite signs, the denominator may approach zero and unrealistic values may be predicted.

For a simple beam $2L = 400$ mm; box section, $2B = 200$ mm, $2H = 25$ mm, $T_f = 1$ mm, $T_w = 10$ mm; load case *I*—uniform load $q = 10$ N mm^{-1} (max $M_y = 200$kNm), load case II—concentrated load at midspan $P = 1$ kN (max $M_y = 100$ kNm), the empirical formula, eqn (4), gives $\lambda^{\mathrm{I}} = 0.670$ and $\lambda^{\mathrm{II}} = 0.514$. From beam theory using flange effective width, $\sigma_x(\lambda^{\mathrm{I}}) = 36.9$ MPa and $\sigma_x(\lambda^{\mathrm{II}}) = 21.4$ MPa. From eqn (8a) $\lambda^{\mathrm{I+II}} = 0.61$. The FEM result for this load combination is $\lambda^{\mathrm{I+II}}_{\mathrm{FEM}} = 0.60$. The agreement is very good. However, with different B/L and E/G ratios the error of eqn (8a) may be greater than the one shown in Table 2, due to accumulation.

6.3. *Complex cross sections*

In the case of complex cross sections (multiple webs, box or U with overhangs, etc.) Moffatt and Dowling (1978) suggested division of the cross section into basic units and estimating the effective width of each one. If the unit represents an overhang, its effective width is to be reduced by 15%.

For a simple beam, uniform load, *U* cross section with overhangs (Fig. 13a) FEM analyses are carried out with the model in Fig. 4. The following modifications of the boundary conditions are introduced:

- on line B_f–B'_f (Fig. 4, in Fig. 13b it is a dot) there are no prescribed zero displacements along y (it is not a symmetry line for the cross section);
- on line A–A' there are prescribed zero displacements along y (it is the symmetry line for the cross section);
- line B_w–B'_w has prescribed equal x displacements with the line U–U', whose position is determined by the B_1/B_2 ratio.

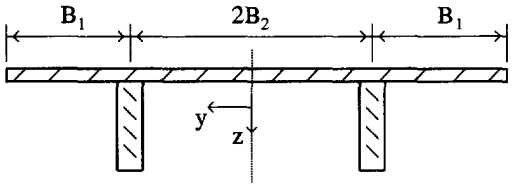

(a)

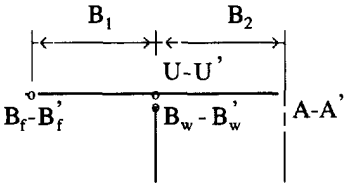

(b)

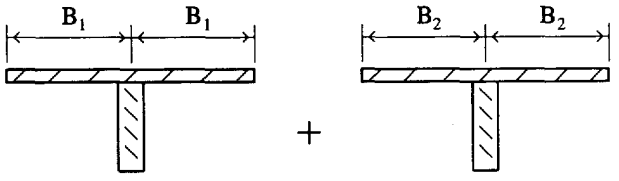

(c)

Fig. 13. (a) U cross section with overhangs; (b) a half section for the FEA. Lines B_f–B_f', ..., etc. defined in Fig. 4; (c) the U section divided into two basic units.

The case $B_1/B_2 = 1$, $E/G = 2.5$ is analyzed for varying B/L from 0.1 to 1.0.

The shear lag coefficient at the overhang is about 15% smaller than the one at the flange between the webs, as already observed by Moffatt and Dowling (1978). The U cross section with overhangs may be divided into two basic units with T cross section, as shown in Fig. 13b. When $B_1/B_2 = 1$ the two basic units are identical. FEA showed that the shear lag in the basic unit is within 15% difference. The shear lag in the overhang is underestimated and the one in the flange between the webs is overestimated. When the whole section is considered the two errors tend to cancel out.

Based on these observations it is proposed to compute the shear lag coefficient for a complex cross section as:

$$\lambda = \frac{\Sigma \lambda_i B_i}{\Sigma B_i}, \tag{9}$$

where λ_i and B_i are the shear lag coefficient and the flange width of each basic unit, respectively.

The accuracy of eqn (9) is compared with FEM results for several test problems. The errors, as defined by eqn (5), are given in Table 5. The $(B_1 + B_2)/L$ ratio has been varied from 0.1 to 1.0 in 20 steps.

Table 5. Errors (%) of the shear lag coefficient λ, eqns (4) and (9). for a cross section with overhangs

E/G	2.5			25.0		
B_1/B_2	1/3	1	3	1/3	1	3
min $\Delta\lambda$ %	−2.5	−5.0	−1.9	−3.0	−6.3	−2.8
max $\Delta\lambda$ %	0.1	1.5	5.7	0.3	4.0	0.7

7. CONCLUSIONS

An extensive FEM study on the shear lag in beams with wide flanges has been performed. Based on the FEM results, an empirical formula has been established for computing the shear lag coefficient λ, ($\lambda = B_e/B$). Several boundary conditions have been considered explicitly. The accuracy is good and error bounds are given.

The application of the formula has been extended to beams with longitudinal stiffeners, load combinations and complex cross sections. A thin plate with stiffeners may be considered as a T-beam with a thin flange.

The primary contribution of the paper is that the presented empirical formula may be used for shear lag calculation in fibre reinforced laminated composite plates with stiffeners which exhibit high values for the E/G ratio and small values for the T_f/T_w ratio.

Acknowledgement—The work reported here was performed at University of Oslo, Department of Mathematics, Mechanics Division, thanks to one year Post-Doctoral research fellowship ST.60.61.222052 given by the Norwegian Research Council (NTNF) to the author. The assurance of Professor J. Hellesland, Professor M. Nygård (University of Oslo, Department of Mathematics) and Dr A. Echtermeyer (Det Norske Veritas Research AS) that it is of practical importance and their discussions on the topic is acknowledged. The author is much obliged to Professor J. Hellesland and all the staff at the University of Oslo for providing excellent working conditions.

REFERENCES

Abdel-Sayed, G. (1969). Effective width of steel deck-plate in bridges. *J. Struct. Div. ASCE* **95,** 1459–1474.

Chang, S. T. (1992). Prestress influence on shear-lag effect in continuous box-girder bridge. *J. Struct. Engng ASCE* **118,** 3113–3121.

Chang, S. T. and Yun, D. (1988). Shear lag effect in box girders with varying depth. *J. Struct. Engng ASCE* **114,** 2280–2292.

Det Norske Veritas (1991). Tentative rules for classification of high speed and light craft. In: *Hull Structural Design, Fibre Composite and Sandwich Constructions*, Part 3, Chap. 4. Det Norske Veritas Classification A/S.

Dezi, L. and Mentrasti, L. (1985). Nonuniform bending-stress distribution (shear lag). *J. Struct. Engng ASCE* **111,** 2675–2690.

Evans, H. R. and Taherian, A. R. (1977). The prediction of shear lag effect in box girders. *Proc. Inst. Civ. Engrs* Part 2, **63,** 69–92.

Foutch, D. A. and Chang, P. C. (1982). A shear lag anomaly. *J. Struct. Engng ASCE* **108,** 1653–1658.

Hinton, E. and Hewitt, A. H. (1975). Program for the analysis of box girder bridges using quadrilateral finite elements, highway engineering computer branch, department, of the Environment, Report HECB/B/14 (QUEST).

Horie, Y., Usuki, S. and Watanabe, N. (1984). A few remarks on the shear lag analysis and the effective width of box girder bridge. *Civil Engng Pract. Des. Engrs* **3,** 569–586.

von Karmán, T. (1924). *Beitrage zur Technischen Mechanic and Technischen Physik, Agust Föppl Festschrift*, pp. 114–127. Springer, Berlin.

Kristek, V. and Evans, H. R. (1985). A hand calculation of the shear lag effect in unstiffened flanges and in flanges with closely spaced stiffeners. *Civil Engng Pract. Des. Engrs* **4,** 163–190.

Kristek, V. and Studnicka, J. (1991). Negative shear lag in flanges of plated structures. *J. Struct. Engng ASCE* **117,** 3553–3569.

Malcom, D. J. and Redwood, R. G. (1970). Shear lag in stiffened box girders. *J. Struct. Div. ASCE* **96,** 1403–1419.

Moffatt, K. R. and Dowling, P. J. (1972). Parametric study on the shear lag phenomenon in steel box girder bridges. Imperial College, London, CESLIC report BG17.

Moffatt, K. R. and Dowling, P. J. (1975). Shear lag in steel box girder bridges. *Struct. Engng* **53,** 439–448.

Moffatt, K. R. and Dowling, P. J. (1978). British shear lag rules for composite girders. *J. Struct. Div. ASCE* **104,** 1123–1130.

Reissner, E. (1941). Least work solutions of shear lag problems. *J. Aeronaut. Sci.* **8,** 284–291.

Roark, R. J. and Young, W. C. (1975). *Formulas for Stress and Strain*, 5th Edn. Section 7.12, McGraw-Hill, New York.

Song, Q. G. and Scordelis, A. C. (1990a). Shear-lag analysis of T-beam, I-beam, and box beams. *J. Struct. Engng ASCE* **116,** 1290–1305.

Song, Q. G. and Scordelis, A. C. (1990b). Formulas for shear-lag effect of T-beam, I-beam and box beams. *J. Struct. Engng ASCE* **116,** 1306–1318.

Tenchev, R. T. (1994). Using membrane elements in a 3D problem—a FEM modeling challenge. *Finite Element News* **3,** 36–42.

Thein Wah (Ed.) (1960). *A Guide for the Analysis of Ship Structures*, pp. 370–391. Office of Technical Service, U.S. Department of Commerce, Washington, DC.

Timoshenko, S. P. and Goodier, J. N. (1970). *Theory of Elasticity*, 3rd Edn, Section 95, pp. 262–267. McGraw-Hill, New York.

Vendhan, Ch.P. and Bhattacharyya, S. K. (1987). A critique of von Karmán's analysis of effective width of panel in bending *Q. J. Mech. Appl. Math.* **40,** 493–505.

Winter, G. (1943). Stress distribution in and equivalent width of flanges of wide, thin-wall steel bridges. Technical Note 893, National Advisory Committee on Aeronautics.